Collagen V Haploinsufficiency Results in Delayed Healing and Altered Wound Matrix Post-Injury in Murine Tendons

Carlson JA[1], Sun M[2], Adams SM[2], Weiss SN[1], Birk DE[2], Soslowsky LJ[1]
[1]McKay Orthopaedic Research Laboratory, University of Pennsylvania, Philadelphia, PA, [2]University of South Florida, Tampa, FL

Disclosures: Carlson JA (N), Sun M (N), Adams SM (N), Weiss SN (N), Birk DE (N), Soslowsky LJ (N)

INTRODUCTION: Patients with Classic Ehlers-Danlos syndrome (*c*EDS), a disorder characterized most commonly by *COL5A1* haploinsufficiency, suffer from tissue hyperelasticity, skin hyperextensibility, tendon/ligament fragility and abnormal wound healing[1,2]. Collagen V (ColV) haploinsufficiency leads to abnormal tissue development and altered collagen assembly, and mechanical loading of the mouse patellar tendon shows a delay in healing[3] and alterations in stiffness and dynamic modulus post-injury[4]. Furthermore, human studies have shown that females have decreased collagen synthesis[5] and altered gene expression during repair[6], likely influencing the healing potential of *c*EDS tendons. Therefore, the objective of this study was to determine the effect of ColV deficiency in female mice on wound matrix formation and resultant structure-function relationships when mechanical load is applied post-injury. We hypothesized that ColV deficiency will have effects post-injury, resulting in increased fibril diameter and cellularity, decreased mechanical properties and leading to a delayed healing response when compared to wild-type tendons.

METHODS: Adult female wild-type (WT) C57/BL6 and heterozygous ***Col5a1***$^{+/-}$ mice, a model for *c*EDS, at 120 days of age (n=84) were used (IACUC approved). Mice were randomly divided into uninjured and injured groups, with injured mice undergoing bilateral patellar tendon injury surgery as described[7]. Injured mice were sacrificed early in the proliferative phase at 1-week (1w), early in the remodeling phase at 3-weeks (3w) or later in remodeling at 6 weeks (6w), and uninjured age-matched mice were also sacrificed. Uninjured and injured patellar tendons of both genotypes were assessed. *Gene Expression:* Real-time PCR was done as described[8]. Each sample (n= 4) was run in duplicate and data was analyzed using StepOne software v2.0. *Transmission Electron Microscopy (TEM):* Samples for TEM analysis of fibril structure (n=4) were fixed *in situ* and processed as described[9]. *Mechanics:* The patella-patellar tendon-tibia complexes were dissected and prepared for mechanical testing (n=12)[10]. Tendons were subjected to a viscoelastic testing protocol containing 3 stress relaxations followed by frequency sweeps, culminating in a ramp-to-failure. Dynamic collagen fiber realignment was quantified using cross-polarization imaging during the ramp-to-failure[10]. *Histology*: Histological sections of the patellar tendon-bone complex (n=4) were prepared using standard techniques. Cellularity was calculated using a standard grading scale. *Statistics:* Two-way ANOVAs with post-hoc Bonferroni tests were used to assess the effects of genotype and time on gene expression. Two-way repeated measures ANOVAs with post-hoc Bonferroni tests were used to assess the changes in realignment for increasing strain levels. Kruskal-Wallis non-parametric one-way ANOVA followed by post-hoc Dunn's test for multiple comparisons were used for histologic data. Significance was set at $p \leq 0.05$.

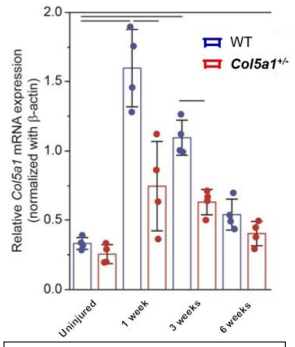

Figure 1: *Col5a1* expression increases 1w and 3w PI in WT but not in ***Col5a1***$^{+/-}$ tendons. Solid lines denote significance.

RESULTS: *Col5a1* expression was significantly increased in WT tendons at 1w and 3w post-injury (PI) compared to uninjured controls. However, no significant changes in *Col5a1* expression were seen following injury in ***Col5a1***$^{+/-}$ tendons (Fig. 1). Genotypic differences in *Col5a1* expression were seen at 1w and 3w PI (Fig. 1). Fibrils from the mid-substance of WT and ***Col5a1***$^{+/-}$ tendons are shown in Figure 2A, with injured tendons having a dominant population of smaller diameter fibrils. Uninjured WT and ***Col5a1***$^{+/-}$ distributions were comparable (data not shown), however, distinctly different distributions for WT and ***Col5a1***$^{+/-}$ fibrils PI were seen, with ***Col5a1***$^{+/-}$ fibrils being larger and more broadly distributed (Fig. 2B). Further, WT and ***Col5a1***$^{+/-}$ tendons realigned through 5% strain, with ***Col5a1***$^{+/-}$ tendons continuing to realign through 6% strain (Fig. 3A). Lastly, significant differences in cellularity (Fig. 3B) were seen between uninjured and both 1w and 3w samples in both genotypes, and between 1w and both 3 and 6w samples, with no difference between genotypes at any time-point. ***Col5a1***$^{+/-}$ tendons had a significant increase in cellularity persisting to 6w PI when compared to uninjured tendons (Fig. 3B).

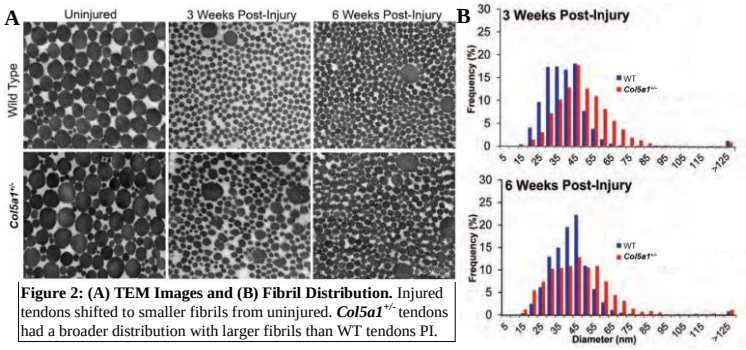

Figure 2: (A) TEM Images and (B) Fibril Distribution. Injured tendons shifted to smaller fibrils from uninjured. ***Col5a1***$^{+/-}$ tendons had a broader distribution with larger fibrils than WT tendons PI.

DISCUSSION: ColV plays a key role in fibrillogenesis, matrix remodeling and response to injury, affecting the structure and function of healing tendon. The lack of an increase in *Col5a1* expression 1w PI in ***Col5a1***$^{+/-}$ tendons would affect all stages of later healing and indicates a reduction in regulation of fibrillogenesis throughout healing. WT *Col5a1* expression returns to uninjured and ***Col5a1***$^{+/-}$ levels by 6w PI injury, indicating that the early increase affects fibril diameter, mechanical properties and cellularity throughout healing. Without the initial increase in ColV following injury, fibrillogenesis is less regulated, resulting in a broader distribution of fibril diameter and a shift to larger fibrils of ***Col5a1***$^{+/-}$ tendons PI, which explains the delayed realignment and is supported by previous work[11]. Following injury, a shift towards smaller fibrils was expected as these are new fibrils from collagen secreting myofibroblasts to fill the injury void. Additionally, increased cellularity in ***Col5a1***$^{+/-}$ tendons would alter the matrix alignment and architecture, weakening the tissue and affecting mechanical properties. The persistence of increased cellularity in ***Col5a1***$^{+/-}$ tendons to 6w PI is consistent with viscoelastic[3] and fatigue data[4], which indicates a delayed healing response in ***Col5a1***$^{+/-}$ tendons. Qualitative comparisons to male data show ***Col5a1***$^{+/-}$ fibril distribution was similar to WT and cellularity returned to uninjured levels by 6w PI, unlike the data shown, indicating that sex affects outcomes of reduction in ColV[12]. Future directions may include later healing time points to better understand the extent of the delayed healing.

SIGNIFICANCE: This study indicates that the lack of an early increase in *Col5a1* expression PI in ***Col5a1***$^{+/-}$ tendons influences matrix architecture, alignment, and cellularity throughout tendon healing, demonstrating altered and delayed healing compared to WT tendons,

REFERENCES: [1] Steinmann et al. *Conn Tissue, Heritable Disorders.* 2002. [2] Wenstrup et al. *J Biol Chem.* 2006. [3] Carlson et al. ORS 2020. [4] Carlson et al. ORS 2019. [5] Ainsworth et al. *CORR.* 1993. [6] Hart et al. *CORR.* 1998. [7] Beason et al. *J. Biomech*, 2012. [8] Sun et al. *Am J Pathol.* 2015. [9] Dunkman et al. *Matrix Biol.* 2013. [10] Kjaer et al. *J. Anat.* 2006. [11] Robinson et al. *Matrix Biol*. 2017. [12] Johnston et al. *JOR.* 2018.

ACKNOWLEDGEMENTS: *This study was supported by NIH/NIAMS AR065995 and the Penn Center for Musculoskeletal Disorders (AR069619).*

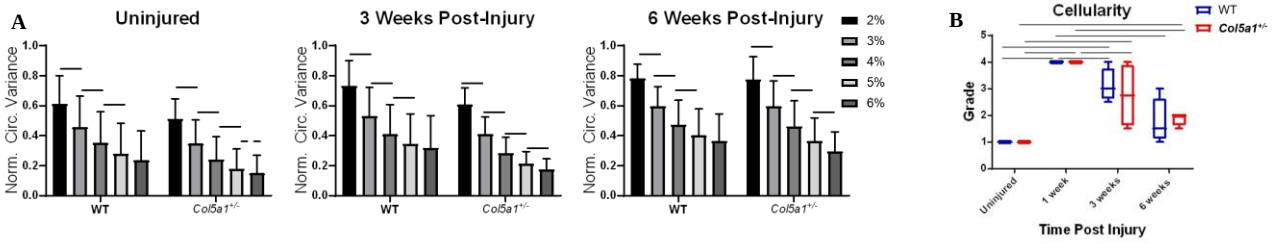

Figure 3: (A) Midsubstance Fiber Realignment. ***Col5a1***$^{+/-}$ uninjured and injured tendons realign through 6% strain, while WT realign through 5% strain. **(B) Cellularity.** Tendons of both genotypes increased significantly in cellularity 1 and 3w PI when compared to uninjured, this increase persisted to 6w PI in ***Col5a1***$^{+/-}$ tendons. Differences in cellularity were also seen between 1w and both 3 and 6w PI in both genotypes. Solid lines denote significance.

Collagen XII Regulates Tendon Dynamic Mechanical Properties and Collagen Fiber Realignment

Ashley K. Fung[1], Nathaniel A. Dyment[1], David E. Birk[2], Louis J. Soslowsky[1]
[1]McKay Orthopaedic Research Laboratory, University of Pennsylvania, Philadelphia, PA
[2]Department of Molecular Pharmacology and Physiology, University of South Florida, Tampa, FL
afung@seas.upenn.edu

Disclosures: Ashley K. Fung (N), Nathaniel A. Dyment (N), David E. Birk (N), Louis J. Soslowsky (N)

INTRODUCTION: Myopathic Ehlers-Danlos syndrome (mEDS) is a connective tissue disorder caused by mutations in the *Col12a1* gene, which encodes for collagen XII, a fibril-associated collagen with interrupted triple helices (FACIT). Patients with mEDS experience myopathy and joint hypermobility and contractures [1], indicating dysregulation of connective tissue function due to the absence of collagen XII. Our recent data showed that tendons from global collagen XII knockout (*Col12a1*$^{-/-}$) mice exhibited disrupted tendon fiber organization and assembly as well as increased cross-sectional area and stiffness. This suggests that the disruption of tendon structure-function in the absence of collagen XII may be caused by a lack of distinct fiber domains resulting in reduced fiber sliding and increased stiffness. However, our previous findings may be confounded by the effects of collagen XII knockdown on other tissues, such as muscle and bone, and the isolated role of collagen XII on tendon mechanical function is still unknown. Therefore, the objectives of this study are to (1) evaluate the specific role of collagen XII in regulating tendon mechanical properties and the dynamic loading response in mature mice using tendon-targeted (scleraxis Cre) collagen XII knockout mice and (2) determine if the role of collagen XII is sex-specific. We hypothesized that collagen XII knockout would lead to increased tendon stiffness and reduced collagen fiber realignment under loading due to disruptions in tendon matrix assembly in both sexes.

METHODS: Patellar tendons from female and male, day 60 tendon-targeted collagen XII knockout (KO) mice (ScxCre;*Col12a1*$^{f/f}$, n=6-8/group) and control (Cre- littermates, n=4-6/group) mice (IACUC approved) were mechanically evaluated using viscoelastic and dynamic collagen fiber realignment methods, as described [2]. Tendons underwent a loading protocol of three stress relaxations at 3, 4, and 5% strain each with a dynamic frequency sweep (0.1, 1, 5, 10Hz), followed by a quasi-static ramp to failure. During the ramp, images were continuously acquired through rotating cross polarizers to evaluate dynamic collagen fiber realignment. For each sex, comparisons between genotypes were made using two-tailed, t-tests with significance set at $p \leq 0.05$ and trends at $p \leq 0.1$.

RESULTS: Cross-sectional area was not different between female KO and control mice, while male KO tendons were smaller than control (**Fig 1a**). Contrary to our hypothesis, linear stiffness was significantly reduced in KO mice for both sexes (**Fig 1b**), and only female KO tendons exhibited a trending decrease in elastic modulus with no difference between male groups (**Fig 1c**). Additionally, percent relaxation was significantly reduced in female KO tendons at all strain levels (5% strain shown in **Fig 1d**). Intriguingly, despite only minor differences in elastic modulus, both sexes demonstrated striking differences in dynamic properties. Compared to their respective controls, dynamic modulus was significantly reduced in KO groups while phase shift was significantly elevated across all strain levels and frequencies (5% strain, 1Hz shown in **Fig 1e** and **f**, respectively). This suggests alterations in matrix structure leading to more viscous mechanical behavior during dynamic loading in the KO groups. This finding is further supported by a reduced degree of collagen fiber realignment (**Fig 2a**) in the female KO group, as shown by increased circular variance at all strain values (**Fig 2b**), and a reduced rate of fiber realignment in the male KO group (**Fig 2c**), as shown by increased circular variance at lower strain values (**Fig 2d**).

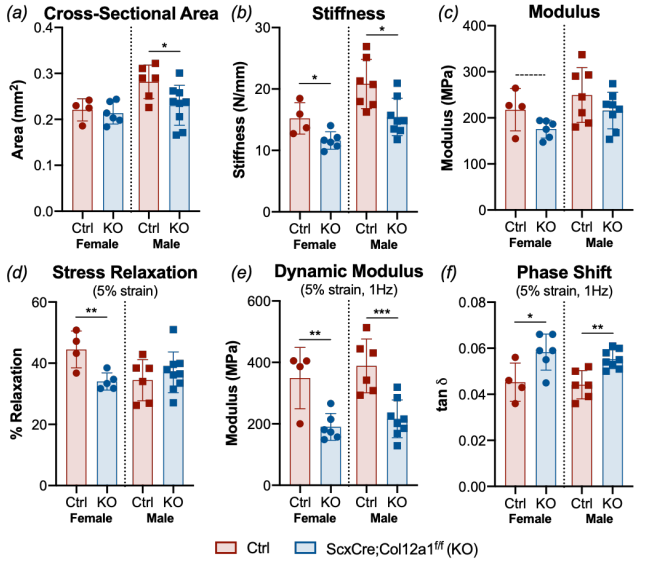

Figure 1: Male KO patellar tendons had (a) reduced cross-sectional area, while both sexes exhibited (b) reduced tendon stiffness. (c) Modulus and (d) percent relaxation were reduced in female KO tendons. (e) Dynamic modulus was reduced and (f) phase shift was elevated in KO groups for both sexes. Data presented as mean ± standard deviation. (---p≤0.1, *p≤0.05, **p≤0.01, ***p≤0.001)

DISCUSSION: This study investigated the isolated role of collagen XII on tendon mechanical function using female and male ScxCre;*Col12a1*$^{f/f}$ mice. Interestingly, KO patellar tendons had reduced stiffness, which contrasts the increased stiffness observed in flexor digitorum longus (FDL) tendons of global collagen XII knockout mice. This suggests that the effects of global knockout of collagen XII on muscle [3] and bone [4] may indirectly affect tendon, necessitating the use of this tendon-targeted mouse model. The effects of collagen XII knockout could also be tendon-specific, as mEDS patients present with both distal joint hypermobility and proximal joint contractures. Furthermore, female KO tendons exhibited less stress relaxation at all strain levels, suggesting alterations in the ability to effectively dissipate load. This could be attributed to a disruption in the establishment of proper hierarchical assembly leading to a reduction in fiber and fibril sliding. Matrix disorganization could also explain the striking differences in dynamic properties, as evidenced by reduced dynamic modulus, increased phase shift, and reduced collagen fiber realignment. Interestingly, our preliminary data shows that, in addition to its structural role, collagen XII may also be critical for regulating cellular organization necessary for establishing hierarchical structure and tendon function, and studies are ongoing to investigate these temporal roles of collagen XII throughout development. Finally, though similar trends were observed for both female and male groups in response to collagen XII knockout, there was a more pronounced effect in female mice. *Coll12a1* polymorphisms have been linked to an increased incidence of ACL ruptures in women [5], suggesting a possible sex-specific effect. Together, our study demonstrates that collagen XII knockout in tendons affects tendon matrix structure and organization, resulting in altered structural, viscoelastic, and dynamic collagen fiber realignment properties.

SIGNIFICANCE: This study demonstrates the critical role of collagen XII in regulating tendon dynamic mechanical behavior, highlighting its importance in establishing tendon structure-function and its re-establishment following injury.

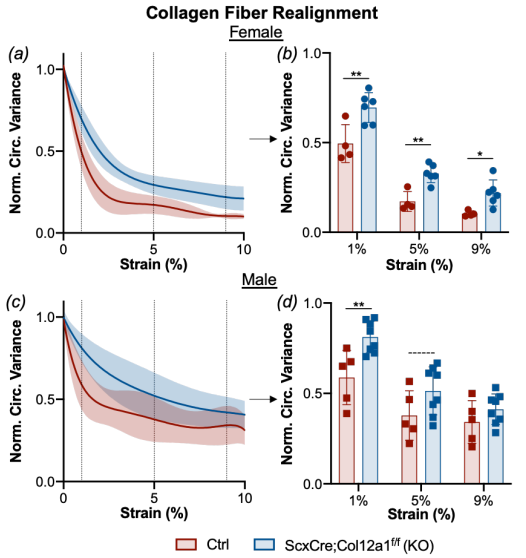

Figure 2: (*a*) Female KO tendons exhibited reduced collagen fiber realignment with increasing strain, as evidenced by (*b*) increased normalized circular variance at all strain levels compared to control. (*c*) Male KO tendons exhibited a reduced rate of collagen fiber realignment with (*d*) increased normalized circular variance at lower strain values compared to control. Data presented as mean ± standard deviation. (---p≤0.1, *p≤0.05, **p≤0.01)

REFERENCES: [1] Punetha et al. *Muscle Nerve* 2017. [2] Dunkman et al. *Matrix Biol*. 2013. [3] Zou et al. *Human Molecular Genetics* 2014. [4] Izu et al *J Cell Biol.* 2011 [5] Posthumus et al. *Br J Sports Med* 2010.

ACKNOWLEDGEMENTS: We thank Dr. Mei Sun for her assistance. This study was funded by NIH/NIAMS T32AR007132 and the Penn Center for Musculoskeletal Disorders (P30AR0696919).

Application of a Fast Fourier Transform-Based Analysis Method to Ultrasound Imaging of the Rat Achilles Tendon

Thomas P. Leahy[1], Snehal S. Shetye[1], Louis J. Soslowsky[1]
[1]McKay Orthopaedic Research Laboratory, University of Pennsylvania, PA
tpleahy@seas.upenn.edu.

Disclosures: Thomas P. Leahy (N), Snehal S. Shetye (N), Louis J. Soslowsky (N)

INTRODUCTION: Ultrasound imaging provides a non-invasive, *in vivo* method to assess tendon structure and can be particularly useful for longitudinal studies in animal models. Specifically, ultrasound imaging provides a speckle pattern generated by the reflectance of sound waves off the extracellular matrix components of the tendon. Previous ultrasound image analysis techniques have not been able to detect changes in this speckle pattern that were representative of the underlying matrix.[1] While fast Fourier transform (FFT)-based analysis algorithms have been shown to distinguish ultrasound characteristics in human patients,[2,3] it is unknown whether this method can be applied to imaging of rat Achilles tendon due to their smaller tendon size and the higher resolution ultrasound transducer used for small animal imaging. Therefore, the objective of this study was to apply and validate an FFT-based analysis technique to ultrasound images of rat Achilles tendons to detect changes in matrix organization. Our hypothesis was that FFT-based parameters would be altered by increases and decreases in matrix organization induced via mechanical loading and injury, respectively.

METHODS: To validate that ultrasound imaging and subsequent FFT-based image analysis could detect changes in rat Achilles tendon matrix organization, mechanical load or induced injury was applied to create increases or decreases in matrix organization, respectively. Loading Study: We previously demonstrated that increasing mechanical load can be used as a proxy for increasing matrix organization via cross-polarizer imaging and second harmonic generation (SHG) microscopy.[1,4] A loading system was manufactured to function within the ultrasound imaging set-up (Fig. 2A). Uninjured Achilles tendons from male 5.5-month-old F344 rats (n=8) were dissected and mounted into the loading system. Quasi-static loads of 0, 2.5, 5, 10, 15, 20, and 25 N were applied to the tendon and simultaneously imaged at each of those load increments. Injury Study: Tendon injury was used as a method for decreasing matrix organization by creating blunt transections on the right Achilles tendon of 5.5-month old F344 rats (n=9; IACUC approved). Rats were anesthetized and placed within the ultrasound imaging system and imaged prior to injury as well as 1, 3, and 6-week post-injury. Rats were then sacrificed at 6-weeks post-injury and the Achilles tendon was imaged with SHG to confirm ultrasound analysis findings. Ultrasound Imaging: A Vevo LAZR ultrasound system (Visualsonics; Toronto, ON) paired with a 40MHz transducer was used to collect ultrasound images during all imaging sessions. Each tendon sample was imaged in the sagittal plane while scanning the transducer across the width of the tendon. Image Analysis: For each sample analysis, 4 representative images were selected to be analyzed using a custom MATLAB script (Mathworks; Natick, MA). Within each image, the tendon was manually cropped and divided into 32x32 pixel square kernels and the FFT of each kernel was computed and high-pass filtered (Fig 1). To describe the frequency spectrum, the magnitude of the largest frequency component represented was output as a percent of the total frequency spectrum (maximum frequency). In addition, an ellipse was fit to the spectrum and the major to minor axis ratio of the ellipse (axis ratio) was reported. Physiologically, these parameters represent the strength of the primary fiber alignment and the uniformity of the fiber alignment across the kernel, respectively. These parameters are reported as averages over all kernels of the tendon. Statistics: Parameters from both the loading and injury studies were analyzed using a repeated measures one-way ANOVA and Tukey's post-hoc tests (significance at $p<0.05$).

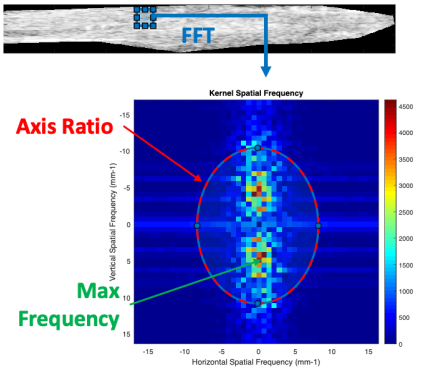

Figure 1. The image analysis process computes the FFT of each square kernel and outputs the maximum frequency and axis ratio as parameters to describe the frequency spectrum.

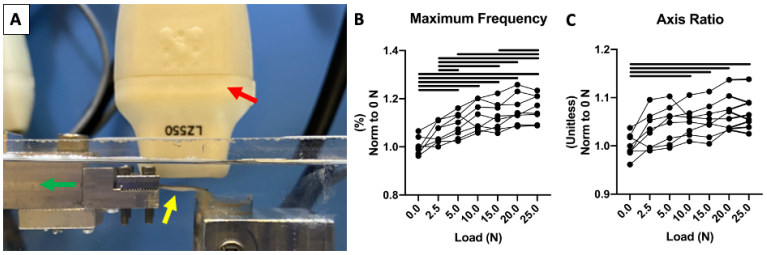

Figure 2. The ultrasound loading study and results. (A) The ultrasound load device, consisting of a 40 MHz transducer (red arrow) imaging the tendon (yellow arrow) while mechanical load is being applied (in the direction of the green arrow). Both **(B) maximum frequency** and **(C) axis ratio** significantly increase with increasing mechanical loading. Solid bars represent significant differences ($p < 0.05$).

RESULTS: As expected, increasing matrix alignment due to mechanical load was detected with significant increases in both maximum frequency (Fig. 2B) and axis ratio (Fig. 2C). Conversely, decreased matrix organization resulting from injury was detected by decreases in both maximum frequency (Fig. 3A) and axis ratio (Fig. 3B). Interestingly, the maximum frequency parameter showed lasting decreases at 6-weeks post-injury. This lasting decrease is consistent with decreased signal intensity in SHG imaging within the injury region of these tendons at 6-weeks post-injury (Fig. 3C).

DISCUSSION: Consistent with our hypothesis, FFT-based analysis of ultrasound images was able to detect both increases in matrix organization due to loading and decreases in matrix organization resulting from injury. Moreover, the changes in FFT-based parameters under these paradigms were in the expected direction given their physiological interpretation discussed within METHODS. Overall, the application of this analysis method to rat Achilles tendon ultrasound represents a scientific advancement as its results are independent of the ROI size and shape, which is in contrast to previous methods.[1] Instead, it detects changes in the ultrasound speckle pattern itself within consistent-sized square kernels, which suggests that the detected changes are representative of changes in the matrix itself. In addition, the parameters reported here are echogenicity-independent, which makes them particularly advantageous for longitudinal studies as echogenicity may change between imaging sessions.

SIGNIFICANCE: This study validated use of an FFT-based analysis technique for ultrasound imaging of the rat Achilles tendon by confirming that it could detect both increases and decreases in matrix organization. This technique will be used to evaluate matrix organization in *in vivo* longitudinal studies.

ACKNOWLEDGEMENTS: We acknowledge support from NIH-funded Penn Center for Musculoskeletal Disorders (P30AR069619) and the Ultrasound Research Services within the Small Animal Imaging Facility research core at the University of Pennsylvania.

REFERENCES: 1. Riggin et al., J Biomech Eng, 2014; 2. Pearson et al., J Biomech, 2017; 3. Kulig et al., Ultrasound Med Biol, 2016; 4. Freedman et al, J R Soc Interface, 2018;

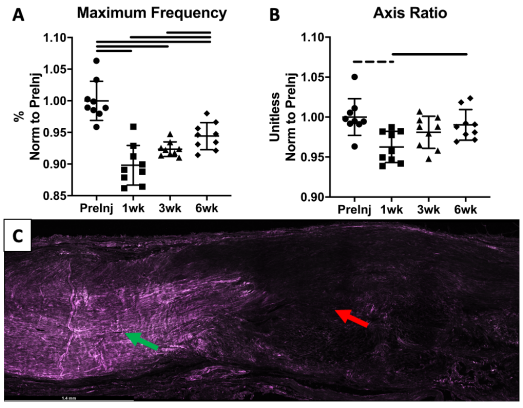

Figure 3. Injured tendon ultrasound analysis revealed that both **(a) maximum frequency** and **(b) axis ratio** were decreased following injury, and maximum frequency remained decreased at 6 weeks. Solid bars represent significance ($p < 0.05$); dashed bars represent trends ($p < 0.1$). **(C) SHG imaging** confirms that at 6-weeks post-injury the injured region of the tendon (red arrow) has lasting deficiencies in tendon matrix structure as evidenced by the low SHG signal compared to the uninjured region of the tendon (green arrow).

Collagen V Knockdown during Phases of Tendon Healing Differentially Impacts Gene Expression

Ryan J Leiphart[1], Brittany L Taylor[1], Stephanie N Weiss[1], Nathaniel A Dyment[1], Louis J Soslowsky[1]
[1]McKay Orthopedic Research Laboratory, University of Pennsylvania, Philadelphia, PA

Disclosures: RJ Leiphart (N), BL Taylor (N), SN Weiss (N), NA Dyment (N), LJ Soslowsky (N)

INTRODUCTION: Classic Ehlers-Danlos Syndrome (cEDS) is a connective tissue disorder often caused by mutations in *COL5A1*, which encodes the primary collagen V alpha chain [1]. Surprisingly, acute *Col5a1* knockdown at the time of murine tendon injury mitigated the quasi-static mechanical deficits of healing tendons [2]. This effect on mechanical parameters was reversed and diminished with *Col5a1* knockdown during the late inflammatory and early remodeling phases of tendon healing, respectively [3]. While this demonstrates that the timing of *Col5a1* knockdown during tendon healing differentially impacts tendon mechanics, the genetic mechanisms underlying this regulation remain unknown. Therefore, the objective of this study was to define the effect of acute *Col5a1* knockdown throughout the phases of tendon healing on injured tendon gene expression. Based on prior mechanical findings, we hypothesized that *Col5a1* knockdown at the time of tendon injury would lead to diminished inflammatory expression and an earlier increase in matrix remodeling gene expression. We hypothesized that this effect would be reversed with *Col5a1* knockdown in the late inflammatory phase, leading to increased inflammatory expression at later healing timepoints. We also hypothesized that *Col5a1* knockdown in the early remodeling phase would cause negligible changes in gene expression.

METHODS: Animals: Male wild-type (WT) (n=20) and bitransgenic *Col5a1*$^{flox/+}$ (n=34) and *Col5a1*$^{flox/flox}$ (n=34) mice with a tamoxifen (TM)-inducible *ROSA-CreER*^{T2} were used (IACUC approved). At 120 days old, mice received bilateral, full thickness, partial width patellar tendon injuries [4]. Mice received two consecutive daily doses of TM (2mg/40g body weight) for Cre-mediated excision of the *Col5a1* gene, resulting in I-*Col5a1*$^{+/-}$ and I-*Col5a1*$^{-/-}$ mice. The first TM injections were administered on the day of injury (WT, TM0), 5 days post-injury (TM5), or 21 days post-injury (TM21) for *Col5a1* knockdown during the different phases of tendon healing. Mice were sacrificed at 1 week (WT, TM0), 3 weeks (WT, TM0, TM5), or 6 weeks (WT, TM0, TM5, TM21) post-injury. Healthy WT control mice received TM doses (3 days of 4mg/40g body weight) at 120 days old and were sacrificed 30 days later. At sacrifice, right patellar tendons were dissected and immediately flash frozen at -80ºC. Gene Expression: For RNA extraction, patellar tendons were thawed in RNA*later* ICE. Tendons were homogenized with plastic pestles in TRIzol and vortexed. RNA was extracted (Direct-zol RNA Microprep, Zymo), and cDNA was reverse transcribed (High Capacity cDNA RT, Thermo). cDNA was pre-amplified for 15 cycles with Taqman assays for 96 target genes and was loaded into a Fluidigm 96.96 Dynamic Array. The 96 target genes included categories of collagens, non-collagenous matrix, matrix remodeling, cell-ECM proteins, cell markers, inflammatory markers, and housekeepers (*Abl1* and *Rps17*). ΔCt was calculated by subtracting the gene Ct from average housekeeping Ct. Statistics: One-way ANOVAs with Tukey post-hoc tests were used to compare ΔCt values across genotypes within knockdown induction timepoint and healing timepoint. Significance was set at $p \leq 0.05$, and trends were set at $p \leq 0.1$.

RESULTS: I-*Col5a1*$^{-/-}$ tendons had decreased *Col5a1* expression compared to WT tendons at each healing timepoint (TM0: 2.2-fold decrease, TM5: 2.4-fold decrease, TM21: 1.4-fold decrease). I-*Col5a1*$^{+/-}$ tendons had decreased *Col5a1* expression compared to WT tendons at 3 weeks post-injury (1.3-fold decrease, TM0 trend). TM0: I-*Col5a1*$^{+/-}$ (trend) and I-*Col5a1*$^{-/-}$ tendons had increased *Postn* expression compared to WT tendons at 3 weeks post-injury, which persisted at 6 weeks post-injury for I-*Col5a1*$^{-/-}$ tendons (Fig 1A). At 6 weeks post-injury, I-*Col5a1*$^{+/-}$ (trend) and I-*Col5a1*$^{-/-}$ tendons had increased *Mmp3* expression compared to WT tendons (Fig1B). TM5: At 6 weeks post-injury, I-*Col5a1*$^{+/-}$ and I-*Col5a1*$^{-/-}$ tendons had increased expression of *Aspn*, *Lum*, *Igf1*, *Mmp3*, and *Thbs4* compared to WT tendons (Fig 2). At this timepoint, I-*Col5a1*$^{+/-}$ (trend) and I-*Col5a1*$^{-/-}$ tendons also had increased expression of *Bgn*, *Lox*, and *Mmp2* compared to WT tendons. TM21: I-*Col5a1*$^{+/-}$ and I-*Col5a1*$^{-/-}$ tendons had increased expression of *Thbs4* compared to WT tendons at 6 weeks post-injury (data not shown). I-*Col5a1*$^{-/-}$ tendons had increased *Mmp3* expression compared to WT tendons at 6 weeks post-injury.

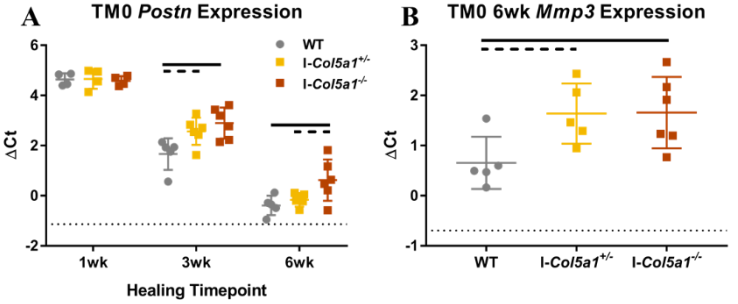

Figure 1. TM0 Gene Expression. (A) I-*Col5a1*$^{-/-}$ tendons had increased *Postn* expression at 3 weeks post-injury that persisted at 6 weeks post-injury. (B) TM0 *Mmp3* expression was increased in collagen V-deficient tendons at 6 weeks post-injury. Dotted lines indicate WT uninjured expression. Solid lines denote $p \leq 0.05$, while dashed lines denote $p \leq 0.1$.

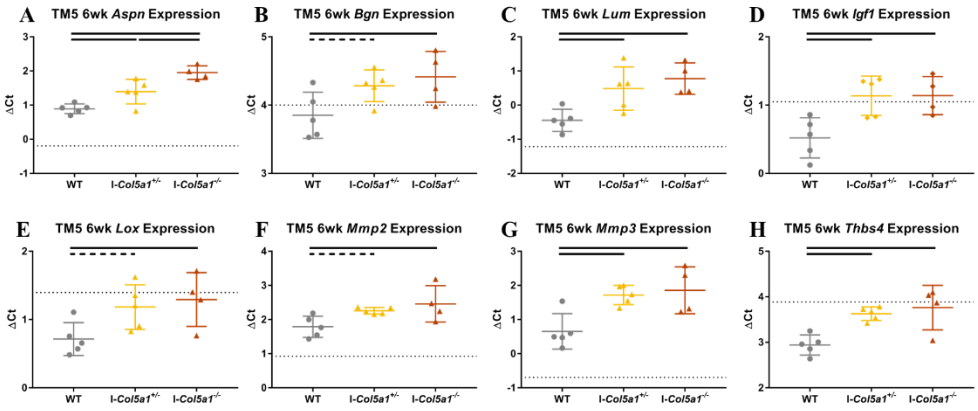

Figure 2. TM5 Gene Expression. At 6 weeks post-injury, *Col5a1* knockdown during the late inflammatory phase of tendon healing lead to increased expression of small leucine-rich proteoglycans (A-C), *Igf1* (D), and matrix remodeling genes (E-H). Dotted lines indicate WT uninjured expression. Solid lines denote $p \leq 0.05$, while dashed lines denote $p \leq 0.1$.

DISCUSSION: Results indicate that collagen V temporally regulates healing tendon gene expression. Effective *Col5a1* knockdown was demonstrated in the *Col5a1*$^{flox/flox}$ model at all healing timepoints. When *Col5a1* was knocked down at the time of injury (TM0), *Postn* and *Mmp3* expression was increased. In addition to increased matrix remodeling expression (*Lox*, *Mmp2*, *Mmp3*, and *Thbs4*), *Col5a1* knockdown during the late inflammatory phase of tendon healing (TM5) led to increased small leucine rich proteoglycan expression (SLRPs, here *Aspn*, *Bgn*, and *Lum*). When *Col5a1* was knocked down during the early remodeling phase of tendon healing (TM21), less robust increases in matrix remodeling espression were observed. The observed expression changes support the mechanical changes seen with *Col5a1* knockdown during different tendon healing phases [2,3]. While *Col5a1* knockdown at the time of injury mitigated mechanical deficits of healing tendons, *Col5a1* knockdown during the late inflammatory phase worsened the mechanical deficits seen with wild-type healing. Compared to TM0 tendons, TM5 tendons exhibited more robust changes in gene expression, including increased SLRP expression. Limitations of this study are the global nature of the *Col5a1* knockdown, which could lead to off-target effects on neighboring tissues, particularly if longer knockdown periods were studied, and the study of gene expression without the addition of protein quantitation. Future work will analyze healing tendon matrix content to define how observed expression changes translate to functional matrix changes.

SIGNIFICANCE: This work elucidates the temporally dynamic role of collagen V on regulating healing tendon gene expression. These results inform which phases of tendon healing are most sensitive to collagen V presence.

REFERENCES: [1] Malfait F et al. *Genet Med*. 2010. [2] Leiphart RJ et al. *ORS Annual Meeting*. 2020. [3] Taylor BL et al. *ORS Annual Meeting*. 2020. [4] Beason DP et al. *J Biomech*. 2012. **ACKNOWLEDGEMENTS**: This work was supported by the NIH (R01AR065995, P30AR069619) and the NSF GRFP.

Collagen V Knockdown in Mature Murine Tendons Causes Sex-Dependent Expression Changes

Ryan J Leiphart[1], Stephanie N Weiss[1], Louis J Soslowsky[1], Nathaniel A Dyment[1]
[1]McKay Orthopedic Research Laboratory, University of Pennsylvania, Philadelphia, PA

Disclosures: RJ Leiphart (N), SN Weiss (N), LJ Soslowsky (N), NA Dyment (N)

INTRODUCTION: Classic Ehlers-Danlos Syndrome (cEDS) is a connective tissue disorder caused by genetic mutations in *COL5A1* [1]. cEDS disproportionately affects females compared to males, and a murine model of cEDS demonstrates sex-dependent changes in tendon mechanical properties with global *Col5a1* haploinsufficiency [2,3]. Further, hormonal differences between sexes are known to cause changes in tendon mechanical properties [4]. It is unknown, however, if the sex-dependent tendon changes in cEDS are driven by developmental and hormonal differences between sexes, or if these changes are a direct result of the sex-dependent role of collagen V in tendon. Therefore, the objective of this study was to isolate the sex-linked role of collagen V in regulating murine patellar tendon gene expression. Based on prior mechanical findings, we hypothesized that induced *Col5a1* knockdown would decrease matrix remodeling gene expression of male tendons but would lead to negligible changes in female tendon gene expression.

METHODS: *Animals:* *Col5a1* gene excision was induced with the tamoxifen-inducible *ROSA26-CreER^{T2}* driver in a dose dependent manner (*Col5a1$^{flox/+}$* and *Col5a1$^{flox/flox}$*) in male and female mice (n=8/genotype/sex) and compared to WT controls (n=6/sex). At 120 days old, mice received three daily TM injections (4mg/40g body weight) for Cre-mediated excision of floxed *Col5a1* alleles, resulting in I-*Col5a1$^{+/-}$* and I-*Col5a1$^{-/-}$* genotypes. Mice were sacrificed 30 days after the first TM injection. Additional *Scx-Cre*;*Col5a1$^{flox/flox}$* mice (n=5/sex) were used to compare *Col5a1* expression and evaluate knockdown efficacy. *Scx-Cre*;*Col5a1$^{flox/flox}$* mice were sacrificed at 150 days old to match the age of experimental mice. At the time of sacrifice, right patellar tendons were isolated and immediately flash frozen at -80ºC. *Gene Expression:* For RNA extraction, patellar tendons were thawed in RNA*later* ICE (Thermo), homogenized with plastic pestles in TRIzol, and further disrupted with vortexing. RNA was extracted (Direct-zol RNA Microprep, Zymo), and cDNA was reverse-transcribed (High Capacity cDNA RT, Thermo). cDNA was pre-amplified for 15 cycles with Taqman assays for 48 target genes and was loaded into a Fluidigm 48.48 Dynamic Array. The 48 target genes fit under broad categories of collagens, non-collagenous matrix, matrix remodeling, differentiation/cell markers, and signaling and inflammation. *Abl1* and *Rps17* were used as housekeeper genes. ΔCt was calculated by subtracting the gene Ct from average housekeeping Ct. *Statistics:* Two-way ANOVAs were used to examine effects of genotype and sex on ΔCt values for each gene. Tukey post-hoc tests were used to compare genotype effects, while Sidak post-hoc tests were used to compare sex effects. Significance was set at $p \leq 0.05$ and trends at $p \leq 0.1$. P-values of two-way ANOVAs are reported below, while p-values of post-hoc comparisons are denoted in the corresponding figures.

RESULTS: *Col5a1* expression was significantly affected by genotype ($p<0.0001$) but not by sex ($p=0.1$) or by interactions between sex and genotype ($p=0.3$). Male I-*Col5a1$^{+/-}$* tendons had a trending decrease in *Col5a1* expression relative to male WT tendons, and male I-*Col5a1$^{-/-}$* tendons had decreased *Col5a1* expression relative to male WT and I-*Col5a1$^{+/-}$* tendons (Fig 1). Female I-*Col5a1$^{-/-}$* tendons had decreased *Col5a1* expression relative to female WT tendons. *Col5a1* expression was not different between *Scx-Cre*;*Col5a1$^{flox/flox}$* tendons and sex-matched I-*Col5a1$^{-/-}$* tendons. Interactions between sex and genotype affected expression of three genes: *Col1a1* ($p=0.02$), *Col11a1* ($p=0.02$), and *Tnc* ($p=0.001$). *Col1a1* expression was decreased in female WT tendons relative to male WT tendons (Fig 2A). Female I-*Col5a1$^{+/-}$* (trend) and I-*Col5a1$^{-/-}$* tendons had increased *Col1a1* expression relative to female WT tendons. *Col11a1* expression was decreased in female WT tendons relative to male WT tendons (Fig 2B). Female I-*Col5a1$^{-/-}$* tendons had increased *Col1a1* expression relative to female WT tendons. Male I-*Col5a1$^{+/-}$* and I-*Col5a1$^{-/-}$* tendons had decreased *Tnc* expression compared to male WT tendons and genotype-matched female tendons (Fig 2C).

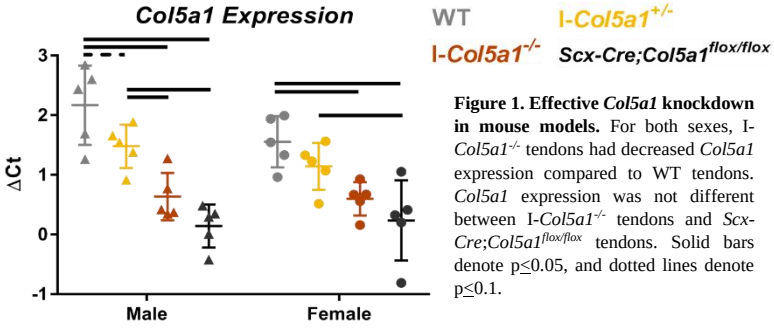

Figure 1. Effective *Col5a1* knockdown in mouse models. For both sexes, I-*Col5a1$^{-/-}$* tendons had decreased *Col5a1* expression compared to WT tendons. *Col5a1* expression was not different between I-*Col5a1$^{-/-}$* tendons and *Scx-Cre*;*Col5a1$^{flox/flox}$* tendons. Solid bars denote $p \leq 0.05$, and dotted lines denote $p \leq 0.1$.

DISCUSSION: A sex-dependent genetic response to *Col5a1* knockdown in mature murine patellar tendons is quantified. I-*Col5a1$^{-/-}$* tendons exhibited *Col5a1* knockdown compared to WT tendons and showed comparable *Col5a1* expression to that of *Scx-Cre*;*Col5a1$^{flox/flox}$* negative control tendons, demonstrating adequate *Col5a1* knockdown for both sexes. In response to *Col5a1* knockdown, male tendons showed decreased *Tnc* expression while female tendons displayed increased expression of *Col1a1* and *Col11a1*. Collagen V regulates collagen I fibrils [5] and is known to interact with tenascin-C [6] and collagen XI [7]. Increased *Col1a1* and *Col11a1* expression in collagen V-deficient female tendons may indicate compensatory expression changes in the absence of collagen V. Contrastingly, decreased *Tnc* expression in collagen V-deficient male tendons suggests that collagen V-deficiency led to reduced expression of other fibrillogenic proteins. The disparate genetic response to *Col5a1* knockdown between male and female mice indicates a sex-dependent role of collagen V in tendon and may explain the sex-linked mechanical outcomes seen in murine models of cEDS [3]. This study is limited by the lack of matrix protein quantification, which would validate the genetic changes observed, and the global nature of the knockdown models. However, the short knockdown window likely minimizes potential off-target and confounding effects of *Col5a1* knockdown on tendon function. Future studies will isolate the sex-dependent role of collagen V in dictating mature tendon mechanical properties.

SIGNIFICANCE: This work isolates and defines the sex-dependent role of collagen V in regulating mature tendon gene expression. Understanding the sex-linked effects of collagen V presence in tendon can inform treatments of disorders such as cEDS.

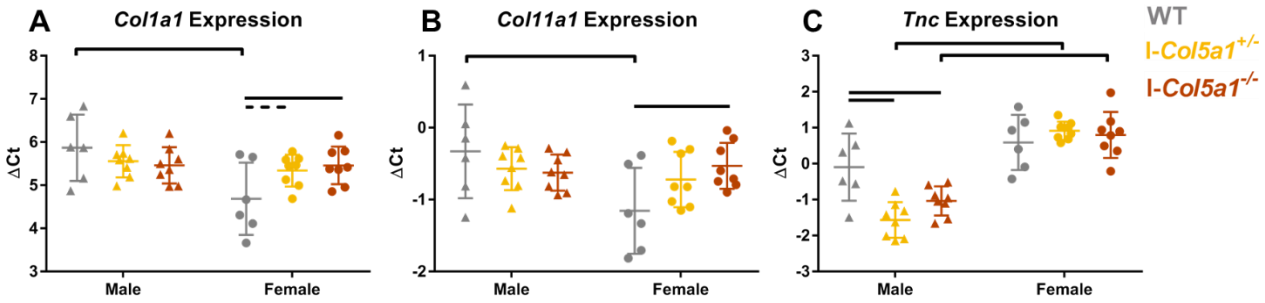

Figure 2. Interactions between sex and genotype affect tendon gene expression. While *Col1a1* (A) and *Col11a1* (B) tendon expression was unchanged across male genotypes, *Col5a1* knockdown led to increased expression of *Col1a1* and *Col11a1* in female tendons. *Col5a1* knockdown led to decreased *Tnc* expression (C) in male tendons but did not alter female *Tnc* expression. Smooth bars denote intra-sex comparisons, while notched bars denote intra-genotype comparisons. Solid bars denote $p \leq 0.05$, and dotted lines denote $p \leq 0.1$.

REFERENCES: [1] Malfait F et al. *GeneReviews*. 2007. [2] Demmler JC et al. *BMJ Open*. 2019. [3] Carlson JA et al. *ORS Annual Meeting*. 2018. [4] Hansen M et al. *Adv Exp Med Biol*. 2016. [5] Wenstrup RJ et al. *J Biol Chem*. 2004. [6] Wenstrup RJ et al. *J Biol Chem*. 2011. [7] Symoens S et al. *Biochem J*. 2011.

ACKNOWLEDGEMENTS: This work was supported by the NIH (R01AR065995, P30AR069619) and the NSF GRFP.

Poly-N-Acetyl Glucosamine (sNAG) is Dose Dependent for Healing of a Rat Rotator Cuff

Nuss CA[1], Huegel J[1], Finkielsztein S[2], Kuntz AF[1], Soslowsky LJ[1]
[1]McKay Orthopaedic Research Laboratory, University of Pennsylvania, Philadelphia, PA
[2]Marine Polymer Technologies, Inc., Burlington, MA

Disclosures: Nuss CA (N), Huegel J (N), Finkielsztein S (3A- Marine Polymer Technologies, Inc.), Kuntz AF (N), Soslowsky LJ (5)

INTRODUCTION: Rotator cuff injuries are a common musculoskeletal problem and frequently require surgical intervention, with repair failure remaining a frequent problem [1]. Many biologic therapies have been utilized in an effort to improve tendon repair [2]. Our previous work demonstrated that 0.2 mg (one 4 mm round) of Talymed (Marine Polymer Technologies, Inc.) material improved tendon-to-bone healing, with treated supraspinatus tendons demonstrating increased maximum load and maximum stress at 4 weeks post-injury compared to saline-treated controls [3]. However, whether an increased dose of this nanofiber material could further improve tendon-to-bone healing after supraspinatus injury is unknown. Therefore, the purpose of this study was to continue to investigate the healing properties of sNAG polymer in a rat rotator cuff repair model, increasing the dose of Talymed (sNAG) delivered at the site of injury and repair. We hypothesized that this increased dose sNAG would improve supraspinatus tendon-to-bone healing compared to saline-treated controls.

METHODS: *Study Design*: 36 adult male Sprague-Dawley rats (400-450g) were used in this IACUC-approved study. All animals underwent bilateral, full thickness transection and repair of the supraspinatus tendon as described [4,5]. Animals were randomized into one of two groups receiving either sNAG or a saline injection (n=18/group). For sNAG treated animals, immediately prior to repairing the supraspinatus, a 0.8 mg dose of the thin sNAG membrane (4 stacked pieces, 4mm diameter) was placed on the "foot print" of the supraspinatus tendon to bone attachment site. All animals were allowed normal cage activity after surgery. Animals were sacrificed either 2 (n=6/group) or 4 weeks (n=12/group) post-injury and repair. Animals sacrificed at 4 weeks underwent longitudinal in vivo ambulatory assessment with measurements pre-injury and 1, 2, and 4 weeks post-injury and repair [6]. *Ex-Vivo*: The right supraspinatus tendons of animals sacrificed at 2 weeks were immediately harvested and processed for histological analysis including quantitative collagen fiber organization analysis [5,8,9]. Animals sacrificed at 4 weeks had their right supraspinatus immediately dissected and processed for histology (n=6/group) and were frozen at -20°C and later thawed for dissection at the time of quasistatic mechanical testing (n=12/group) [7,8]. *Statistics:* Mechanical testing and collagen fiber organization data were evaluated using one-tailed t-tests after confirming data normality. Semi-quantitative histological comparisons were made using Mann-Whitney U tests. Ambulatory assessment comparisons were made using a 2-way ANOVA with repeated measures on time with follow-up t-tests between groups at each time point. Significance was set at $p<0.05$ for all comparisons.

RESULTS**:** *Mechanical properties*: At 4 weeks after injury, there were no differences between saline-treated control and sNAG-treated tendons for cross-sectional area, maximum load, modulus, or stiffness (Fig. 1). *Histologic observations*: Semi-quantitative grading indicated that cellularity was increased with sNAG treatment at the insertion at 4 weeks post-injury (Fig. 2A) and in the midsubstance at 2 weeks post-injury (Fig 2B). There were no differences between groups for cell shape in the tendon insertion or midsubstance (Fig 2 C,D). *Ambulatory Measurements*: sNAG had no effect at any time point on animal stride width, stride length, stance time, rate of loading, propulsion force, or peak vertical force (Fig. 3).

DISCUSSION**:** The purpose of this study was to further investigate the healing properties of an increased dose of sNAG polymer in a rat rotator cuff repair model. Surprisingly, a higher dose did not produce significant improvements in rotator cuff healing as was seen with a previously studied "standard dose" [3]. Although many parameters did not show differences between groups, there were no negative effects with an increased dose of sNAG. Treated tendons did demonstrate increased tendon cellularity, but this did not translate to improved mechanical properties. Another previous study utilizing repeated injections of 0.2 mg of a liquid-formulation of sNAG led to improved Achilles tendon healing 3 weeks after a full thickness, partial width tear [10]. This study suggests that sNAG may be dose-dependent. Early histological changes with this dose could lead to later improvements in tendon strength; further studies are needed to investigate this possibility, as well as to explain the mechanism of action for the changes identified.

SIGNIFICANCE: The effects that sNAG has on rotator cuff tendon healing may be dose-dependent, as the higher dose tested in this study (4x original) did not improve tendon properties.

REFERENCES**:** [1] Galatz LM et al. J Bone Joint Surg Am, 2004. [2] Soslowsky LJ et al. Curr Rheum Rep 2015. [3] Nuss CA et al. Ann Biomed Eng, 2017. [4] Beason DP et al. J Shoulder Elbow Surg, 2012. [5] Connizzo BK et al. Clin Orthop, 2014. [6] Gimbel JA et al. J Biomech Eng, 2007. [7] Sarver JJ et al. J Biomech 2010. [8] Bey MJ et al. J Biomech Eng, 2002. [9] Thomopoulos S et al. J Orthop Res, 2003. [10] Nuss CA et al. ORS Trans 2020, #0757.

ACKNOWLEDGEMENTS**:** Funding was provided by Marine Polymer Technologies, Inc. and the Penn Center for Musculoskeletal Disorders (P30 AR069619). We thank Stephanie Weiss and Harina Raja for their assistance.

IMAGES AND TABLES:

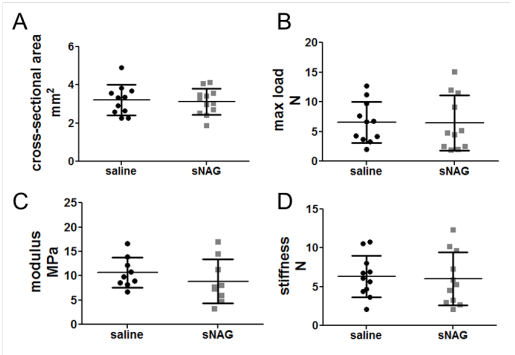

Figure 1. **Mechanical Properties.** Four weeks after injury, there were no differences between saline-treated controls and sNAG-treated tendons for (A) cross-sectional area, (B) maximum load, (C) modulus, or (D) stiffness. Data shown as mean±SD.

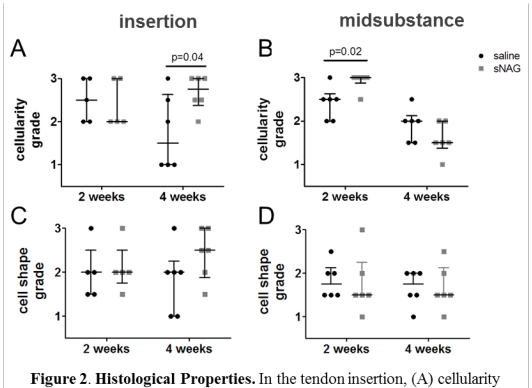

Figure 2. **Histological Properties.** In the tendon insertion, (A) cellularity was increased with sNAG treatment at 4 weeks post-injury. Similarly, in the midsubstance, (B) sNAG increased cellularity at 2 weeks. There were no differences between groups for cell shape (C) in the tendon insertion or (D) midsubstance. Data represented as median±IQR.

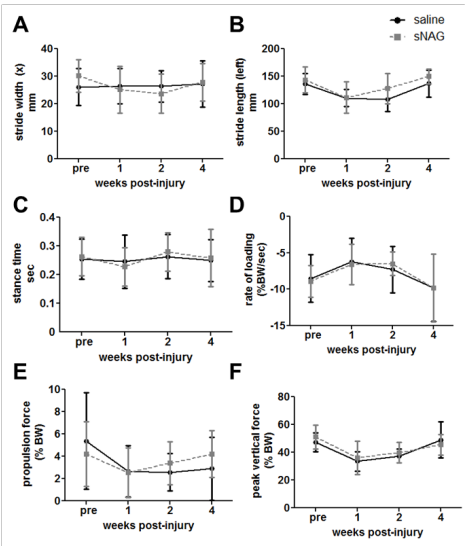

Figure 3. **Gait Properties.** sNAG treatment had no effect at any time point on animal (A) stride width between paws, (B) stride length, (C) stance time, (D) rate of loading, (E) propulsion force, or (F) peak vertical force. Data shown as mean±SD.

Adverse Mechanical Consequences from Abnormal Activation and Deactivation of the mTORC1 Pathway in Tendons

Snehal S. Shetye, Yeonju Lee, Kyu Sang Jeong
University of Pennsylvania, Philadelphia, PA
shetye@pennmedicine.upenn.edu

Disclosures: Snehal S. Shetye (N), YeonJu Lee (N), Kyu Sang Jeong (N)

INTRODUCTION: Tendon, a collagen-rich tissue, is the primary component that transmits loads from muscle to bone. It is relatively avascular and hypocellular, and thus can be afflicted with tendinopathy and ruptures without a clear solution towards complete recovery either via medical treatment or physical rehabilitation. Thus, recent efforts have strived to understand the mechanistic basis of tendon development and maturation, which might help guide better treatment options. The mechanistic target of rapamycin complex 1 (mTORC1) regulates multiple cellular biological processes such as metabolism, growth, proliferation, and survival. Recently, we showed that both deactivation and activation of mTORC1 in tendon caused impaired postnatal tendon development with immature collagen fibrillogenesis, which suggest that fine-tune regulation of mTORC1 signaling is essential for normal postnatal tendon development. While these data highlight the molecular effects of deactivation and activation of the mTORC1 pathways, downstream macroscale effects on tendon mechanical function remain unclear. Therefore, the objective of this study was to examine the mechanical response of mouse Achilles tendons after activation or deactivation of mTORC1, via tendon-specific deletion of *Tsc1* (gain-of-function) or *Raptor* (loss-of-function), respectively. We hypothesized that any deviations from physiological levels of mTORC1 signaling will adversely affect the structural and material properties of tendons, with a pronounced effect due to impaired collagen fibrillogenesis.

METHODS: All procedures were approved by UPenn's IACUC. Mouse hindlimbs (n=10/group) were collected from the *ScxCre;Raptor$^{f/f}$* mice at P60 for loss-of-function study. Mouse hindlimbs (n=7/group) were collected from the *ScxCre;Tsc1$^{f/f}$* mice for gain-of-function study at P30. All mice assigned for mechanical testing were frozen at -20C till the day of testing. Mice were thawed at room temperature and calcaneal bone-Achilles tendon-muscle complexes were grossly dissected. All extraneous soft tissues and muscles were finely dissected, and a custom laser device was used to measure the cross-sectional area (CSA) of the Achilles tendon. The myotendinous junction was sandwiched between two sandpaper tabs with cyanoacrylate glue to prevent any slippage. The calcaneal bone was gripped with a custom fixture and the construct was mounted onto a material testing machine (Instron 5542, Instron Inc., Norwood, MA). All testing was conducted in phosphate buffered saline bath at room temperature. Each sample was preloaded to 0.02N followed by 10 cycles of preconditioning between 0.02 to 0.04N. After a resting period of 60 seconds at 0N the sample was quasi-statically ramped to failure at a strain rate of 0.03%/s. All data were collected at 100Hz. Ensuing force-displacement curves were analyzed to obtain failure load (N) and tissue stiffness (N/mm, defined as the slope of the linear region). Cross-sectional areas (mm2) and gauge length (mm) values were used to obtain stress-strain curves for each sample. Modulus (MPa) was calculated as the slope of the linear region of the stress-strain curve and failure stress (N/mm^2) as the maximum stress value observed.

RESULTS: Consistent with previous histological study, Achilles tendons from *ScxCre;Raptor$^{f/f}$* mice had structural deficits with a significantly reduced cross-sectional area (CSA) [Fig.1A]. This further resulted in a significantly reduced failure load [Fig.1B] and significantly lower tendon stiffness [Fig.1C]. *ScxCre;Raptor$^{f/f}$* tendons did not show material deficits with no significant differences observed in tendon modulus [Fig.1D] and failure stress (data not shown). Consistent with previous histological study, Achilles tendons from *ScxCre;Tsc1$^{f/f}$* did not have any macroscale structural changes with no significant difference in tendon CSA [Fig.2A]. Unexpectedly, structural properties including failure load [Fig.2B] and tendon stiffness [Fig. 2C] were significantly lower. Further, material effects were evident in *ScxCre;Tsc1$^{f/f}$* tendons with a significantly reduced tendon modulus [Fig.2D] and a trending difference ($p<0.1$) in failure stress (data not shown).

DISCUSSION: This study investigated the macroscale mechanical sequelae from abnormal activation and deactivation of the mTORC1 pathway in murine Achilles tendons. Each of these perturbations resulted in substantial, but interestingly divergent disruption of tendon mechanical response. Our previous work with *ScxCre;Raptor$^{f/f}$* tendons showed the loss of the typical bimodal fibril diameter distribution with abrogation of all large diameter fibrils. Surprisingly, this resulting unimodal distribution of smaller diameter fibrils did not affect the material properties of these tendons with not differences observed in tendon modulus or failure stress. Transmission electron microscopy of *ScxCre;Tsc1$^{f/f}$* tendons showed a more severe effect on collagen fibrils with most diameters in the 40-50nm range. Further, histological analysis depicted a very disorganized matrix and increased neovascularization. These structural and ECM disruptions may explain the significant material property effects seen here in *ScxCre;Tsc1$^{f/f}$* tendons. However, it was surprising that even with these ECM deficiencies, macroscale structure *i.e.,* cross-sectional area was not affected. Future studies will explore microscale structural changes in tendon ECM via second harmonic generation imaging of collagen fibrils, and atomic force microscopy imaging to measure fibril sliding and deformation, which might explain the macroscale mechanical response reported here.

SIGNIFICANCE/CLINICAL RELEVANCE: The findings reported here suggest that *optimal* mTORC1 signaling is crucial for postnatal tendon development and abnormal activation or deactivation has deleterious effects on tendon mechanics. Clinically, temporal control of this pathway might allow for improved tendon healing outcomes.

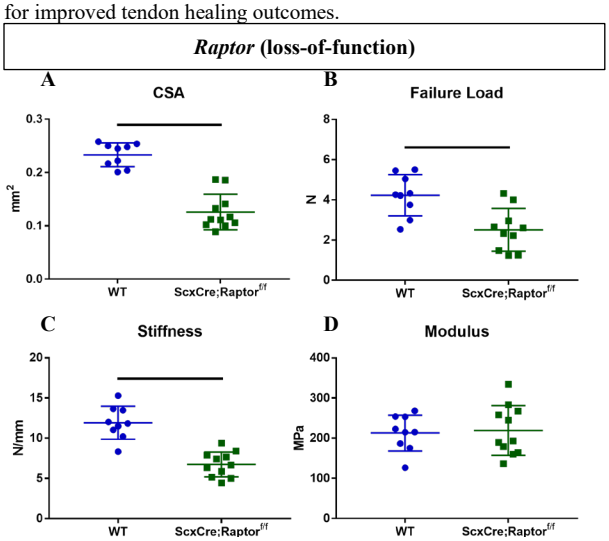

Figure 1 - Comparison of mechanical properties of control and *ScxCre;Raptor$^{f/f}$* mouse Achilles tendons **(A)** Cross-sectional area (CSA) **(B)** Failure load **(C)** Stiffness **(D)** Modulus. Bars indicate a significant difference at $p<0.05$ after unpaired two-tailed t-tests.

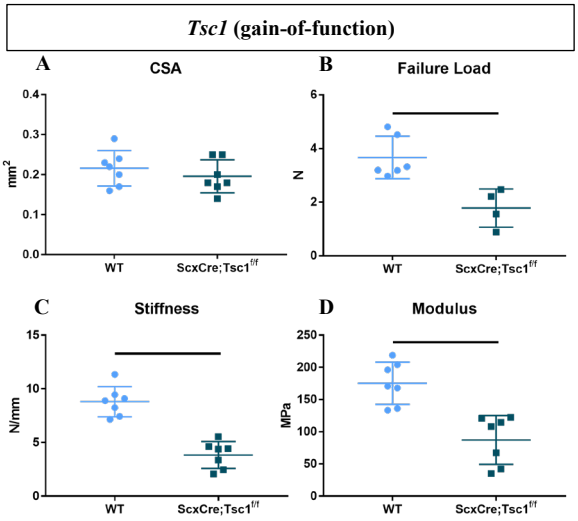

Figure 2 - Comparison of mechanical properties of control and *ScxCre;Tsc1$^{f/f}$* mouse Achilles tendons **(A)** Cross-sectional area (CSA) **(B)** Failure load **(C)** Stiffness **(D)** Modulus. Bars indicate a significant difference at $p<0.05$ after unpaired two-tailed t-tests.